RF PARTICLE SEPARATORS

M. Bell, P. Bramham, R. D. Fortune, E. Keil, B. W. Montague

CERN

(Presented by B. W. MONTAGUE)

INTRODUCTION

The spatial separation of high energy particles with different rest masses by means of radio-frequency fields exploits the time-resolving properties of such fields to discriminate between the velocities of different particle types having a common momentum. Such separation is possible up to much higher momenta than can be achieved with conventional electrostatic separators. RF separation schemes have been discussed by Panofsky [1], Veksler [2], Hereward [3], Blewett [4] and Good [5]. Phillips [6] and Panofsky [7] describe the deflection of a bunched beam of 350 MeV/c electrons by RF fields in a microwave cavity. In December 1959 Panofsky gave a talk at CERN (unpublished note), in which he proposed a microwave RF separator using two relatively short deflecting waveguides excited in a circularly polarised mode. This proposal, apart from the circular polarisation, formed the basis of the RF separator design described by Schnell [8] and now under construction at CERN. A summary of RF separator studies at CERN and elsewhere up to 1961 is given by Geiger et al. [9]. Since then, RF separators have been studied at Berkeley, Brookhaven, CERN, Stanford and possibly elsewhere. Hahn [10] has described some of the Brookhaven work, and Murray [11] made a preliminary investigation of an «accelerator type» separator. Since much of this work has so far appeared only in internal reports we shall not attempt to give a complete bibliography.

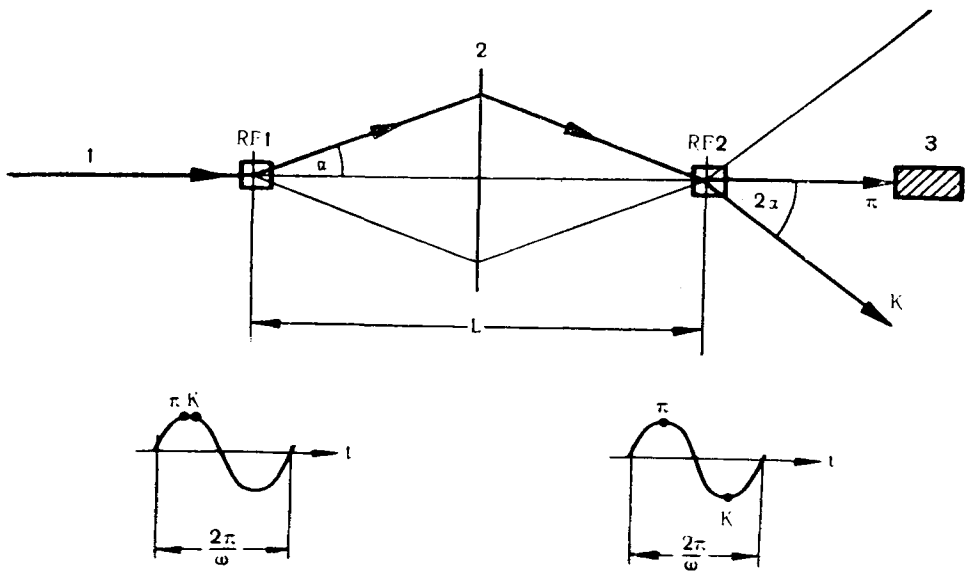

Fig. 1.

1 — momentum analysed beam; *2* — lens system; *3* — beam stopper.

PRINCIPLES OF AN RF SEPARATOR

The essential features of RF separation can conveniently be illustrated by a simplified model of the CERN separator. In Fig. 1,

a momentum-analysed pencil beam of mixed particles passes successively through two similar RF deflecting cavities, RF1 and RF2, spaced a distance L apart. Mid-way between the cavities is a lens system which images RF1 to RF2. The relative phasing of power in the two cavities is adjusted so that one particle, a pion say, arrives in the two deflectors successively at the same RF phase.

In the case illustrated, a pion and a kaon with the same momentum arrive in the first cavity at the peak of the wave and both receive the full deflection $+\alpha$. In the second cavity the pion again receives a deflection $+\alpha$ which, due to the negative unity magnification of the system, cancels the initial deflection and brings the pion back on the axis. The kaon, with a velocity slightly less than that of the pion, arrives in RF2 at a later phase of the RF. In the most favourable case there is a phase slip of π between the two particle types, and the initial deflection of the kaon is doubled. For the full range of entry phase the pions are all brought back to the axis whereas the kaons emerge in a fan-shaped distribution with semi-angle 2α. A centrally placed beam stopper then intercepts all the pions and some kaons, allowing most of the kaons to pass either side.

In contrast to the Panofsky proposal, in which particles are deflected into a cone by a circularly polarised wave, the CERN design deflects only in one plane. This reduces the RF power requirements by a factor of 2, and eases the tolerances on lens aberrations in the plane of momentum separation, perpendicular to the mass separation plane.

The situation shown in Fig. 1, where there is exactly π phase slip between wanted and unwanted particles over the distance L, yields the optimum conditions for separation and occurs when:

$$L = \frac{\lambda_0 (p_0 c)^2}{|W_1^2 - W_2^2|}, \qquad (1)$$

where λ_0 is the RF wavelength (10.5 cm in the CERN separator), W_1 and W_2 are the rest energies of the two particles and p_0 their momentum. We call p_0 the design momentum, commonly referring it to $K - \pi$ separation.

Within certain limitations, the separator can be operated both below and above design momentum, by suitably adjusting RF phase and amplitude. Over the range of operating momentum the two-cavity separator can eliminate only one type of particle, except at (or near) certain momenta where two unwanted particles have a relative phase slip equal to an integral multiple of 2π. To overcome this limitation Schnell [8] proposed using a third deflector cavity, which enables two particle types to be eliminated over the whole momentum range of the separator.

ACCEPTANCE

The simple model just described requires certain elaborations in practice. Although the deflector cavities are «short», in the sense that the relative phase slip between pions and kaons along their length is small, they

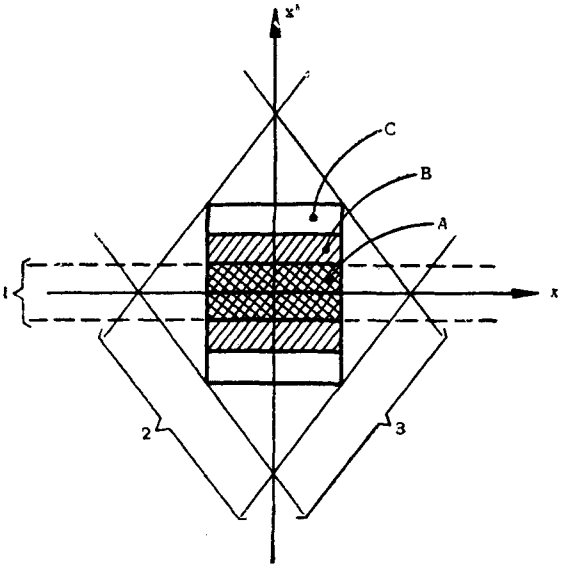

Fig. 2.
1 — beam stopper; *2* — entry limiting lines; *3* — exit limiting lines.

still have a limited acceptance. To exploit fully the acceptance of the two cavities they should be at conjugate foci of the beam transport system between them, which schould have unity magnification. This is conveniently achieved by making it a symmetrical quadrupole triplet or two doublets. The transfer matrix is then

$$\begin{pmatrix} -1 & 0 \\ a_{21} & -1 \end{pmatrix}, \qquad (2)$$

where the a_{21} is different in the two planes and depends on the detailed disposition of the lenses. We have chosen $a_{21} = 0$ in the vertical

plane, thus obtaining a complete cancellation of any possible aberration in the RF deflection of the unwanted particles. The a_{21} in the other plane is then determined.

Fig. 2. shows the mass separation phase plane diagram at the deflection centre of one of the cavities. (It can be shown [12] that a deflector cavity of any length can be represented as a point deflector, by applying a suitable phase plane transformation). The diamond-shaped acceptance area of the cavity is formed by transforming the aperture limits at the two extremities to the centre. The largest rectangle *C* is the maximum area available with relatively simple optics. The incoming beam is shaped in the phase plane by collimators and a quadrupole doublet to occupy the small rectangle *A*. After deflection in RF1 the beam of mixed particles occupies the intermediate area *B*. The transformation (2) rotates Fig. 2 through π in the phase plane, so it remains unchanged in form. The deflection in RF2 acts differently on the two particle types, bringing the pions back into *A* and increasing the kaon deflection to occupy the maximum phase space area *C*. Following RF2 is a doublet system and beam stopper which is the inverse of the incoming beam shaping system, so that the beam stopper transformed back to RF2 covers the area *A* occupied by pions. The central beam stopper, proposed by Montague [12], offers some advantages over conventional collimating techniques with respect to contamination by edge scattered pions. Theoretically it intercepts about 30% of the kaons, but in practice the stopper is made wider to allow for chromatic aberrations of the lens system, tolerances on RF phase and amplitude, Coulomb scattering in the stopper, anisochronism due to momentum bite and beam divergence, and various other imperfections, so that up to 50% of the wanted particles could be lost. The plane perpendicular to that of mass separation is used for momentum analysis, and does not require quite such refined optics.

CERN SEPARATOR PARAMETERS

The basic parameters are shown in Table 1. The frequency was chosen in S-band (10.5 cm) mainly from the availability of high power RF sources, subject to the limitations of equation (1). However, S-band frequencies seem to be close to the optimum for use with a 25 GeV accelerator. Design momentum was chosen to be sufficiently above the practical limit of electrostatic separators to fulfil an obvious need. The available flight path in the CPS East Experimental Area is just sufficient to accommodate these parameters.

Table 1

Nominal frequency (λ_0=10.5 cm)	2856 MHz
Design momentum ($K-\pi$) . .	10.34 Gev/c
Design momentum ($p-\pi$) . . .	20.24 GeV/c
Cavity spacing (L)	50 m
Cavity length	3 m
Cavity half aperture	27 mm
Cavity acceptance (vertical)	4 × 20 mm·mrad
Cavity acceptance (horizontal)	4 × 60 mm·mrad
Peak transverse momentum per cavity	20 MeV/c
Peak RF power per cavity	17 MW

Details of the first RF separated beam combined with an electrostatically separated beam for lower momenta are presented by W. W. Neale at this Conference. Installation of the RF separator is planned for the end of this year. The detailed design of a future improved RF separated beam, using a fast-ejected primary beam from the CPS and a third deflector, is being studied currently.

DEFLECTING STRUCTURE

Each deflecting cavity consists of 3 m of uniform iris-loaded circular waveguide operated in a travelling wave mode. The structure is similar to that of an electron linac, but using a TM_{11} type hybrid mode which provides a transverse deflecting force. This mode was apparently first investigated at Stanford [13], with parameters which showed backward-wave behaviour, and is almost certainly the mode responsible for pulse-shortening in electron linacs [14]. The hybrid mode in circular geometry has been studied in considerable detail at CERN [15, 16], by Garault [17], Hahn [18] and by Hahn and Halama [19]. Gabillard [20] has investigated similar modes in rectangular geometry.

It was found at an early stage of these studies that the mode is a non-degenerate mixture of TM_{11} and TE_{11} waves, and that either a forward or a backward wave can be propagated, depending on the parameters chosen. The CERN design uses a forward wave, since this provides a slightly larger aperture. It brings about a small complication, however, in that the lower branch of the dispersion

curve (Fig. 3) is not monotonic. At the operating frequency two longitudinal modes can be propagated, the wanted one at $v_p = c$ and a spurious one with a negative phase velocity. By proper coupler design this spurious mode can be suppressed to the extent of absorbing negligible power.

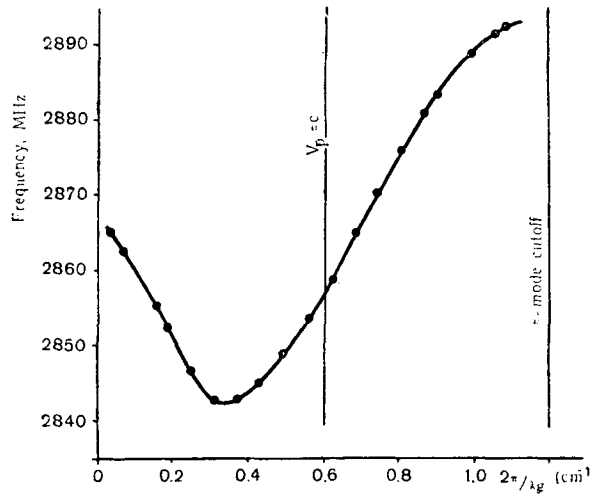

Fig. 3. E_{11}/H_{11} hybrid mode, lower branch.

In an unperturbed circular cylindrical waveguide the polarisation of the mode is arbitrary. If nothing were done to remove the degeneracy, slight imperfections might rotate the deflection plane along the length of the guide. To prevent this, the CERN waveguide (Fig. 4)

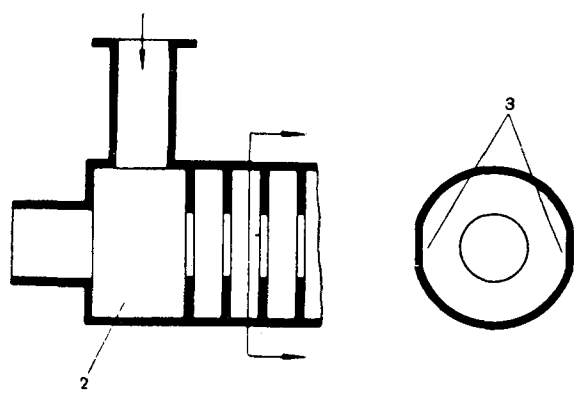

Fig. 4.
1 — radio-frequency; *2* — coupling cell; *3* — mode polarization flats.

has two flats along the cylindrical wall, which split the passbands of the two polarisation components so that, at the correct frequency, only the wanted component will be synchronous with the particles. The waveguide is made in 1-metre lengths by the electroforming technique, which enables the mode polarising flats to be produced without difficulty.

Each deflector cavity is evacuated to about 10^{-6} Torr by cold-cathode ion pumps, and to reduce the degassing to a minimum the majority of the vacuum joints are metallic, the remainder being in baked-out fluor-elastomer (Viton). Initial pumping down to below 10^{-4} Torr is obtained by a Roots pump backed by a two-stage rotary pump.

Each deflector station can be isolated under vacuum and withdrawn from the beam path, leaving the full 20 cm aperture of the beam transport system available if the RF separator is not in use. In normal operation the high vacuum of the deflector system is isolated from the rough vacuum of the beam transport system by 6-micron windows of polyester (Mylar)

COMPARISON BETWEEN RF AND ELECTROSTATIC SEPARATION

In an electrostatic separator, the difference $\Delta x'$ between the deflections of two types of particles is, in relativistic approximation:

$$\Delta x' = \frac{Es}{pc}\Delta\left(\frac{1}{\beta}\right) = \frac{Es}{2(pc)^3}(W_1^2 - W_2^2), \quad (3)$$

where E is the electric field, s — the separator length, p — the momentum, β — the normalised velocity of a particle, and W_1, W_2 — the rest energies. For the RF separator, one can show that the difference in deflection between two particle types is

$$\Delta x' = \frac{2Es}{pc}\sin\left(\frac{\pi}{2}\cdot\frac{p_0^2}{p^2}\right), \quad (4)$$

where p_0 is the design momentum. In the neighbourhood of p_0 the sine function is close to unity, and $\Delta x'$ varies only as p^{-1}. Comparison of (4) with (3) demonstrates the basic advantage of RF separation; the very small velocity difference term $\Delta\left(\frac{1}{\beta}\right)$ is absent.

At momenta well above p_0, (4) reduces to

$$\Delta x' \approx \frac{Es}{2(pc)^3}(W_1^2 - W_2^2)\frac{2\pi L}{\lambda_0}. \quad (5)$$

Here the variation with momentum is the same as in the electrostatic case, but there is a factor $(2\pi L/\lambda_0)$ which, using microwaves, can give easily three orders of magnitude increased deflection over the electrostatic separator at higher momenta. Additionally, there is the

advantage that field gradients can be higher at microwaves than at dc without sparking occurring.

RF separators have certain drawbacks compared with electrostatic separators. Due to the high RF power required, pulse lengths are at present limited to a few microseconds, making RF separation primarily of interest to bubble chamber beams. Current developments in microwave superconductivity could make possible long pulse or c. w. RF separators and greatly extend the fields of application, in both the medium and high energy region.

With an RF separator working well below design momentum ($p < p_0$), the velocity spread, and hence the anisochronism associated with a non-zero momentum bite, can encroach on the phase separation between wanted and unwanted particles. This sets a lower practical limit to the operating momentum for a given design momentum p_0. (Anisochronism due to beam divergence is fairly small in the CERN design.) The upper limit of momentum ($p > p_0$) is determined by a combination of available RF power and attainable tolerances on amplitude and phase of the RF [21]. Nevertheless, the separator can operate efficiently over a momentum range of at least 2 to 1 without changing L to obtain a different p_0.

RF SEPARATION AT ULTRA-HIGH ENERGIES

In conjunction with design studies for accelerators in the 150—300 GeV range a preliminary study of RF separators for higher energies has been carried out [21, 22]. If one introduces the obvious condition that the deflection of the particles should always be sufficient to fill the cavity acceptance, one can obtain scaling laws in terms of design momentum p_0, RF wavelength λ_0 and deflecting field amplitude E. The scaling laws are:

for cavity spacing L:

$$L \sim \lambda_0 p_0^2, \tag{6}$$

for cavity length s:

$$s \sim \lambda_0^{1/2} p_0^{1/2} E^{-1/2}, \tag{7}$$

for cavity acceptance A:

$$A \sim \lambda_0^{3/2} p_0^{-1/2} E^{1/2}, \tag{8}$$

for the phase velocity solerance between the cavities $\frac{\partial v}{v}$:

$$\frac{\delta v}{v} \sim p_0^{-2}, \tag{9}$$

for the phase velocity tolerance in the cavities $\frac{\delta \omega}{\omega}$:

$$\frac{\delta \omega}{\omega} \sim \lambda_0^{1/2} p_0^{-1/2} E^{1/2}. \tag{10}$$

The amplitude tolerances are independent of all these parameters.

For constant E, the amount of RF power equipment necessary is roughly proportional to s and therefore to $p_0^{1/2}$, thus varying slowly. p_0 enters strongly only in L and $\delta v/v$.

However, it seems likely that in a first stage of development beyond the present CERN separator, ten times tighter tolerances in the phase reference system could be met by fairly straightforward improvements of present-day techniques. Thus RF separators with $p_0 = 30$ GeV/c look feasible, offering K-π separation up to ~ 50 GeV/c and p-π separation up to ~ 100 GeV/c. Their main characteristics are given in Table 2.

Table 2

Parameters of RF Separators for Ultra-High Energies

	Stage I	Stage II
Design momentum p_0	30	100 GeV/c
RF wavelength λ_0	0.1	0.03 m
Cavity spacing L	400	1350 m
Cavity length s	5.5	5.1 m
Cavity acceptance vertical	4×9	4×0.9 mm·mrad
Cavity acceptance horizontal	4×28	4×2.7 mm·mrad
Beam length	1	2 km
Momentum bite	0 1	0.1%
Solid angle	2	0.3 μsr

According to present estimates [23] the fluxes of kaons and antiprotons obtainable with such separators are between 10^3 and 10^4 particles/RF pulse over the whole operating range, from both a 150 and a 300 GeV accelerator. For a further increase of design momentum in a second stage of development, different techniques are required to meet the tolerances of phasing, e. g. 10^{-7} at $p_0 = 100$ GeV/c. The cavity spacing would become excessive if *S-band were still used, as Robertson* [24] has already pointed out.

However, the high particle fluxes quoted above suggest that RF separators with much smaller acceptance can still provide adequate fluxes for bubble chambers. Therefore the RF wavelength can by reduced, thus shortening

both the cavity spacing and the whole length of the beam to reasonable values. At the same time the decay loss ot kaons is reduced so as partly to offset the reduction of acceptance. The parameters of an RF separator using X-band (3 cm wavelength) are also given in Table 2. This separator offers K-π separation up to $\sim$ 150 GeV/c and p-π separation up to $\sim$ 200 GeV/c with fluxes higher than 100 particles/RF pulse for all momenta inside the operating range, if used with a 300 GeV accelerator. The small momentum bite chosen limits to a tolerable level chromatic aberrations, which tend to be rather large for these long beams. It is probably also desirable for nuclear physics reasons. The figures quoted for solid angle take into account chromatic aberrations and aperture limitations of the beam transport equipment associated with the RF separators. This is why they are smaller than values one might expect from the acceptance of the cavities.

CONCLUSION

As far as we know, no high-energy RF separator has yet been completed. It would therefore be unrealistic to suppose that the CERN equipment will go into operation at the beginning of 1964 without some unexpected problems being encountered. However, the potentialities of RF separation are such that it will be worth many months of work perfecting a device which shows such promise both at momenta currently available and for future ultra-high energy accelerators.

REFERENCES

1. Panofsky W. K. H. HEPL-82 (1956).
2. Veksler V. A/Conf. 15/P/2229 (1958).
3. Hereward H. G. CERN PS/Int./TH 58-8 (1958).
4. Blewett J. P. In: Proceedings of the International Conference on High Energy Accelerators (CERN, 1959), p. 422.
5. Good M. L. UCRL-8929 (1959).
6. Phillips P. R. HEPL-171 (1959).
7. Panofsky W. K. H. In: Proceedings of the International Conference on High Energy Accelerators (CERN, 1959), p. 428.
8. Schnell W. CERN 61-5 (1961).
9. Geiger M., Lapostolle P., Montague B. W. CERN 61-26 (1961).
10. Hahn H. CERN/Brookhaven Meeting, Sept. 1962, Minutes p. 103.
11. Murray J. J. In: Proceedings of the Conference on Instrumentation for High-Energy Physics (CERN, 1962), p. 26.
12. Montague B. W. CERN PS/Int. AR/PSep/60-1 (1960).
13. Stanford University Microwave Lab., M. L. Report 581 (1959).
14. Bell M., Bramham P., Montague B. W. Nature, **198**, 4877, 277 (1963).
15. CERN reports in preparation.
16. Bramham P. CERN AR/Int.PSep/63-4 (1963).
17. Garault Y. Comptes rendus, **254**, 8, 1391 and 5, 843 (1962); **255**, 22, 2920 (1962).
18. Hahn H. BNL Acc. Dept. Int. Repts. HH-4, and HH-5 (1962).
19. Hahn H., Halama H. J. BNL Acc. Dept. Int. Rept. HH/HJH-2 (1963).
20. Gabillard R. Inst. Radiotechnique, Lille, IREL 61-1 and 61-2 (1961).
21. Keil E. CERN AR/Int.PSep/63-3 (1963).
22. Keil E. CERN AR/Int. PSep/62-3 (1962).
23. Cocconi G., Koester L. H., Perkins D. H. UCRL-SS 28-2 (1961).
24. Robertson D. S. Brookhaven Report IA-8 (1961).